

Fault detection using acceptance ratio analysis on polycrystalline grid-connected photovoltaics system

Nurmalessa Muhammad^{1,2}, Fiona Roland¹, Hedzlin Zainuddin^{1,2}

¹Department of Physics and Materials, Faculty of Applied Sciences, Universiti Teknologi MARA, Shah Alam, Malaysia

²Solar Photovoltaic Energy Conversion Technology Research and Application (SPECTRA), Universiti Teknologi MARA, Shah Alam, Malaysia

Article Info

Article history:

Received Sep 9, 2022

Revised Jan 5, 2023

Accepted Jan 19, 2023

Keywords:

AC power

Acceptance ratio

Grid-connected

Photovoltaic system

Polycrystalline

ABSTRACT

Around the world, electricity generation from PV photovoltaic systems is increasing, achieving 10-20% PV system efficiency. However, PV systems degrade due to the technology and the operating conditions and become worse in tropical climate countries. Hence, degradation is one of the key performance indicators for the reliability assessment of a PV system. This paper presents the acceptance ratio (AR) analysis grid-connected photovoltaic (GCPV) located on the campus of the Universiti Teknologi MARA, Shah Alam, Malaysia as the key performance indicators. A comparative analysis of the actual and predicted AC Power and AR of the polycrystalline GCPV system is carried out over monitoring of a one-year period. MATLAB software is chosen to simulate the output power using actual data. Malaysian Standard MS2692:2020 has noted that the AR value must ≥ 0.9 to classify as accepted in testing and commissioning tests and AR < 0.9 has been indicated as a non-accepted GCPV system. The results of acceptance ratio (AR), yield (Y), specific yield (SY), and performance ratio (PR) show that almost half of the AR's data results show below 0.9 with the performance ratio of PV systems was less than 75%, indicating that the systems needed to be completely replaced.

This is an open access article under the [CC BY-SA](#) license.



Corresponding Author:

Nurmalessa Muhammad

Department of Physics and Materials, Faculty of Applied Sciences, Universiti Teknologi MARA

40450, Shah Alam, Selangor, Malaysia

Email: nurmalessa@uitm.edu.my

1. INTRODUCTION

On growing environmental issues, solar energy has been widely used due to its inexhaustible and environmentally sustainable benefits [1]–[4]. The primary source of solar energy is called solar power [5]. Due to its reliability and minimal maintenance requirements, a significant number of photovoltaic (PV) systems have been deployed around the world in recent years [5]–[7]. The projected lifespan of the PV modules is typically around 20-25 years [8]. However, due to their unreliable estimation of the module's expected performance, several solar PV modules show poor performance in the field [9], [10].

The factors that contributed to the poor performance of the PV system may be faults or anomalies present in the system [11]–[14]. There have been different kinds of research on fault detection. These studies include fault detection using cables to capture losses using mathematical diagnostic methods [15], output ratio (PR) measurement, voltage, and current observation [16], [17] array and grid power loss analysis [18]–[20], artificial neural network [4], [21]–[23] environment conditions [8], [9], temperature variation [24]–[27] and experimental method [17]. A few other fault detection techniques have been introduced on the

AC side of PV systems, such as hot-spot detection [28], [29] and satellite data [6]. Artificial intelligence (AI) approaches also have been used such as neural networks and the fuzzy classification system [30], [31].

The acceptance ratio (AR), which is defined as the ratio of the actual AC power output to the expected AC power output, is one of the criteria used in recent research to identify problems in PV systems. However, there hasn't been much research done on early fault detection using AR in Malaysia [11], [7]. Based on real and predicted polycrystalline GCPV systems, this study aims to develop a fault detection approach aimed at optimizing the operational efficiency of GCPV systems. To detect the fault, the acceptance ratio (AR) assessment was performed for polycrystalline GCPV systems. Polycrystalline GCPV system are mostly used in entire world, leading a good subject to compare [32], [33]. This study is beneficial to compare the performance of polycrystalline GCPV system in tropical climate country with another climate.

2. METHOD

2.1. Polycrystalline PV plant site description

In this study, a polycrystalline GCPV system was chosen to investigate fault detection. The polycrystalline GCPV systems have a capacity of 5.405 kWp and were installed in April 2012, at the Universiti Teknologi MARA (UiTM) Shah Alam's green energy research center (GERC) test site. The polycrystalline systems have 23 PV modules in total, with 12 series and 11 series in String 1 and String 2, respectively. The system mounting structure is retrofitted onto a metal deck and installed at a 10° angle on the parking rooftop facing South-East. The data loggers were linked to the weather monitoring station and inverter, which recorded environmental and electrical data such as AC power output, solar irradiance, module temperature, and wind speed. Each data point was continuously recorded at five-minute intervals. The historical data of environmental and electrical data from November 2018 to November 2019 were extracted for analysis in this study.

2.2. AC power analysis (P_{ac_actual} and $P_{ac_predict}$)

This section compares actual and predicted AC power. Figure 1 depicts an AC power analysis flowchart. Based on Figure 1, P_{ac_actual} is the actual AC power was drawn from the data logger; meanwhile, predicted AC power, $P_{ac_predict}$ was computed using the mathematical model. $P_{ac_predict}$ can be calculated as (1).

$$P_{ac_predict} = P_{array_STC} \times k_g \times k_{temp} \times k_{mm} \times \eta_{inv} \times \eta_{cable} \times k_{dirt} \times k_{age} \times k_{shade} \quad (1)$$

Where P_{array_STC} is the peak power of the PV array at STC, k_g is peak sun factor (decimal), k_{temp} is the de-rating factor of power due to cell temperature, k_{mm} is the de-rating factor due to module mismatch, η_{inv} is the efficiency of inverter and η_{cable} is the efficiency of cables, k_{dirt} is the de-rating factor due to dirt, k_{age} is the de-rating factor due to aging of the PV module and k_{shade} is the de-rating factor due to shading.

$$k_{age} = \frac{G}{1000} \quad (2)$$

While G is the plane of array irradiance.

$$k_{temp} = 1 + \left[\left(\frac{\delta}{100} \right) \times (T_{cell} - T_{STC}) \right] \quad (3)$$

Where T_{cell} is the cell effective temperature and T_{STC} is the cell temperature at STC (provided in the datasheet) [32].

2.3. Acceptance ratio (AR)

Figure 2 depicts the AR analysis flow chart in this section. AR is commonly defined as the ratio of actual power to predicted AC power. The sustainable energy development authority of Malaysia (SEDA) established an AR threshold value to address the acceptance of a fully installed and operational PV system. An approved operating PV system is said to be the system if the AR value is equal to or greater than 0.9. In other words, there is no fault in the system [32]. To calculate AR for GCPV systems, the following equations must be used:

$$AR = \frac{P_{ac_actual}}{P_{ac_predict}} \quad (4)$$

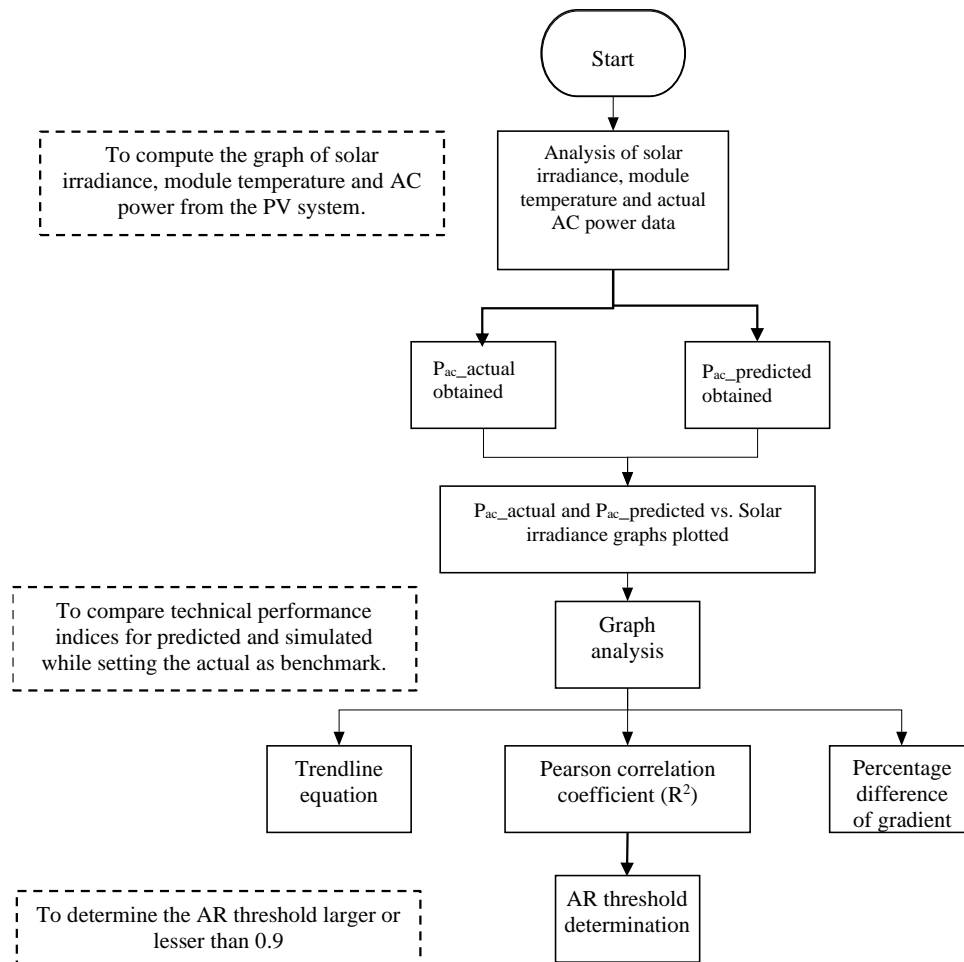


Figure 1. A flowchart for AC power analysis

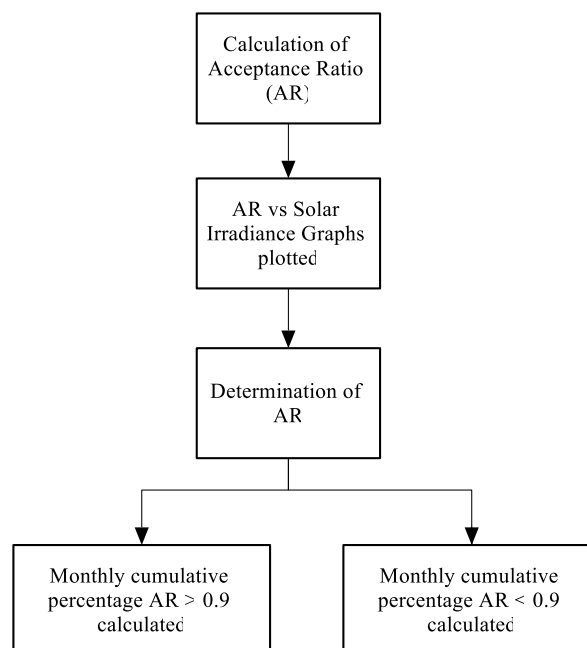


Figure 2. A flowchart for AR analysis

2.4. Yield (Y)

Yield (Y) is the sum of energy that the device produces. Yields are commonly recorded as annual values for PV systems because the usable solar irradiation varies over the year. The monthly yield or daily yield may also be reported [16]. The predicted yield can be calculated as (5).

$$Y_{predict} = P_{array_STC} \times PSH_{poa} \times k_{deration_y} \times \mu_{module} \quad (5)$$

Where $Y_{predict}$ is the predicted energy yield (kWh), and $k_{deration_y}$ is derationed factor of energy yield by year (dimensionless) [16] and can be calculated as (6).

$$k_{deration_y} = k_{mm} \times k_{tem_ave} \times k_{dirt} \times k_{age} \times k_{shade} \quad (6)$$

2.5. Specific yield (SY)

The specific yield is the amount of energy produced by the device per unit capacity. The annual specific yield is frequently reported because available solar irradiation varies throughout the year. It is also possible to report monthly or daily values [16]. The expected specific yields are calculated as (7).

$$SY_{predict} = \frac{Y_{predict}}{P_{array_STC}} \quad (7)$$

Where $SY_{predict}$ is the predicted specific energy yield kWh(kWp)⁻¹, and SY_{actual} is the actual specific energy yield kWh(kWp)⁻¹ [16].

2.6. Performance ratio (PR)

The performance ratio is the dimensional quantity that provides the overall device quality (SEDA, 2014). The actual and predicted performance ratio can be calculated as:

$$PR_{predict} = \frac{Y_{predict}}{Y_{ideal}} \quad (8)$$

$$PR_{actual} = \frac{Y_{actual}}{Y_{ideal}} \quad (9)$$

where $PR_{predict}$ is the predicted performance ratio (decimal), PR_{actual} is actual performance ratio (decimal). While, Y_{ideal} can be calculated as:

$$Y_{ideal} = \frac{P_{array_STC}}{H_{poa}} \quad (10)$$

or

$$Y_{ideal} = \mu_{module} \times P_{array_STC} \times H_{poa} \quad (11)$$

where Y_{ideal} is ideal yield (kWh), μ_{module} is the total area of PV array (m²), H_{poa} is irradiation received on plane-of-array (poa) per annum [16].

3. RESULTS AND DISCUSSION

The analysis and results are divided into two sections: AC power analysis and AR threshold. Except for recordings available at night, all analyses were performed on filtered data. To carry out the investigation, the correlation coefficient was assumed. R^2 is one of the most commonly used correlation coefficients and can measure the linear relationship between two variables. The correlation coefficient between actual and predicted AC power output for each month is shown in Figure 3 to Figure 14. AC power output for each month is depicted in red (actual plot) and blue (predicted plot). R^2 has fluctuated between 0.8 and 0.9 over the years. High coefficients indicate that the actual power is very close to the predicted power, indicating that the PV system is performing admirably. According to Figure 3 to Figure 14, the actual AC power value begins to deviate from the prediction when the solar irradiance exceeds 200 W/m². This inverter failed to operate due to discrepancies between actual and predicted AC power output data.

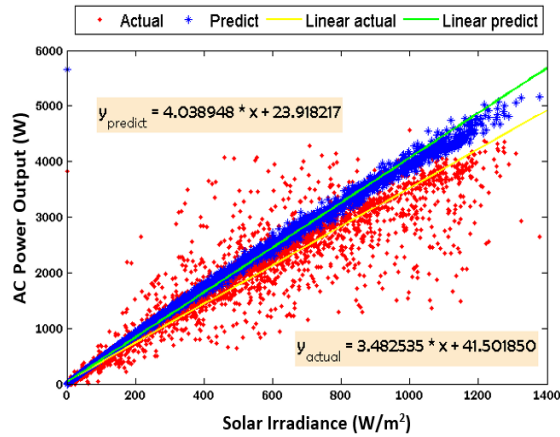


Figure 3. AC power output in relation to solar irradiance for November 2018)

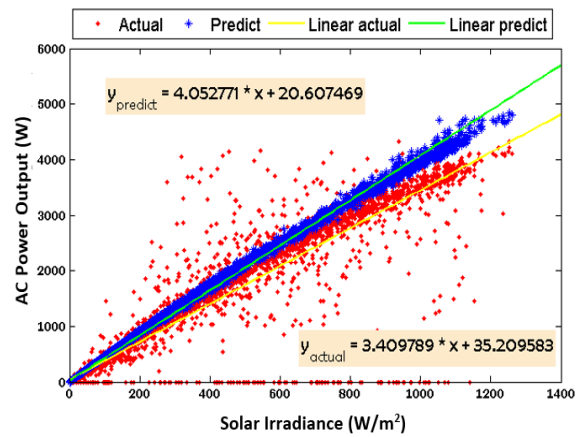


Figure 4. AC power output in relation to solar irradiance for December 2018

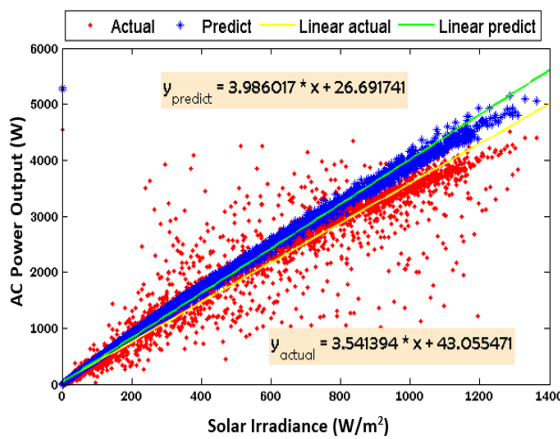


Figure 5. AC power output in relation to solar irradiance for January 2019

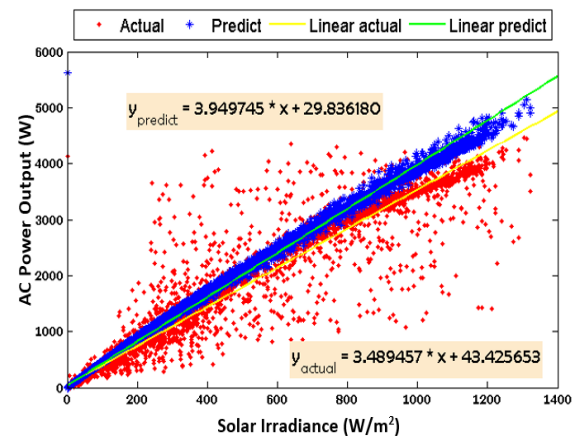


Figure 6. AC power output in relation to solar irradiance for February 2019

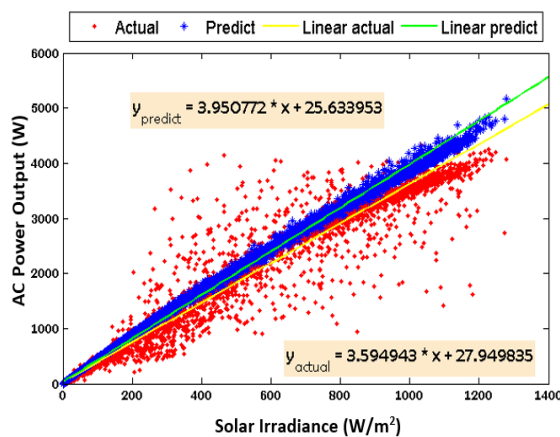


Figure 7. AC power output in relation to solar irradiance for March 2019

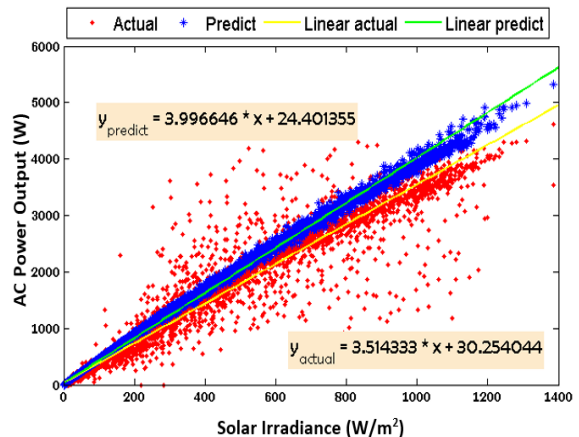


Figure 8. AC power output in relation to solar irradiance for April 2019

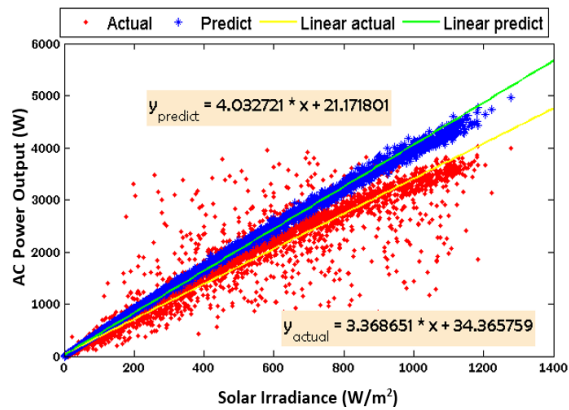


Figure 9. AC power output in relation to solar irradiance for May 2019

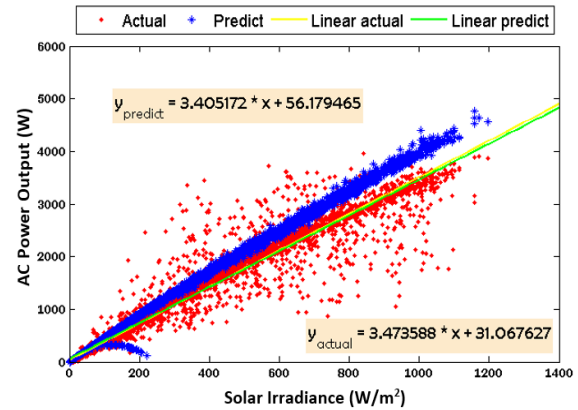


Figure 10. AC power output in relation to solar irradiance for June 2019

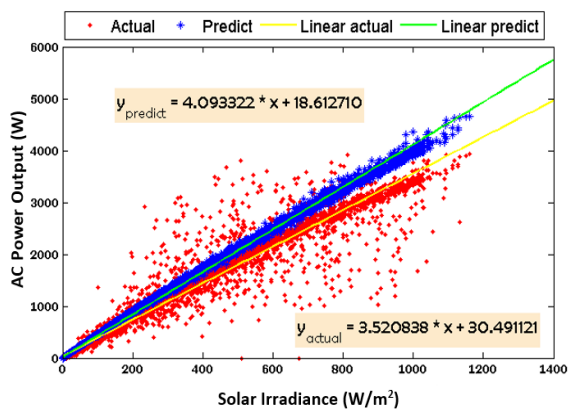


Figure 11. AC power output in relation to solar irradiance for July 2019

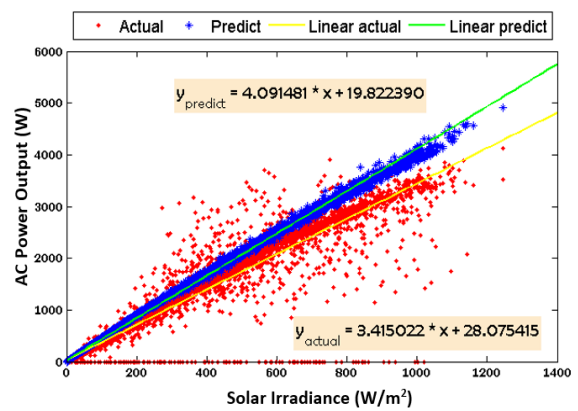


Figure 12. AC power output in relation to solar irradiance for August 2019

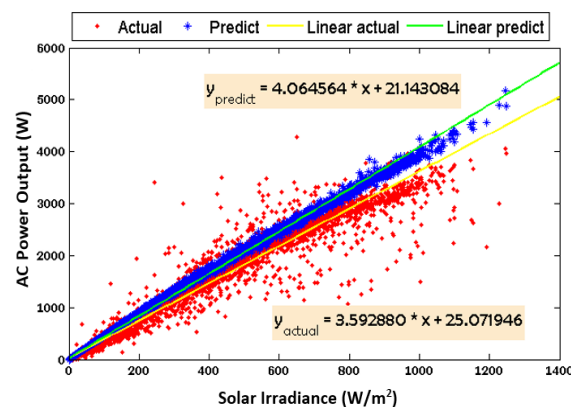


Figure 13. AC power output in relation to solar irradiance for September 2019

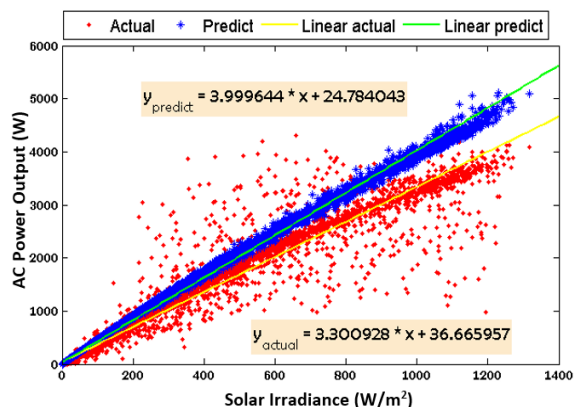


Figure 14. AC power output in relation to solar irradiance for October 2019

3.1. AR threshold

Figure 15 through Figure 26 show the AR for each month. The red color represents the acceptance test's AR threshold of 0.9 (as defined by Malaysian standard MS2692:2020). The results show that a greater amount of data fell below 0.9 in November 2018 and December 2019. The graph shows that half of the data is below, and half is above 0.9 from January 2019 to July 2019. Meanwhile, a graph from August 2019 shows that half of the data is less than 0.9. However, according to the graph in September 2019, half the data

is below and half is above 0.9. Finally, in December 2019, the graph shows that the amount of data is less than 0.9. Overall, the majority of the data shown in the graphs is less than the AR value of 0.9.

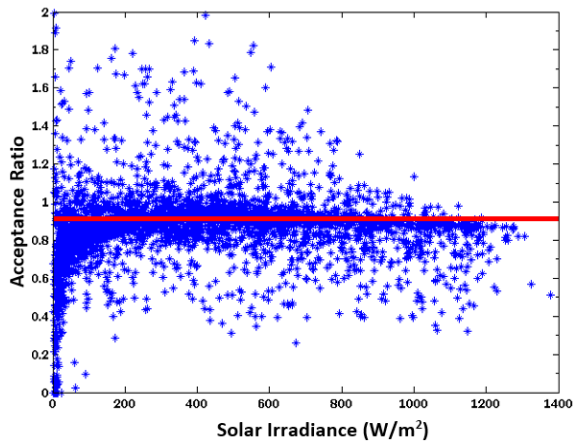


Figure 15. Acceptance ratio in relation to solar irradiance for November 2018

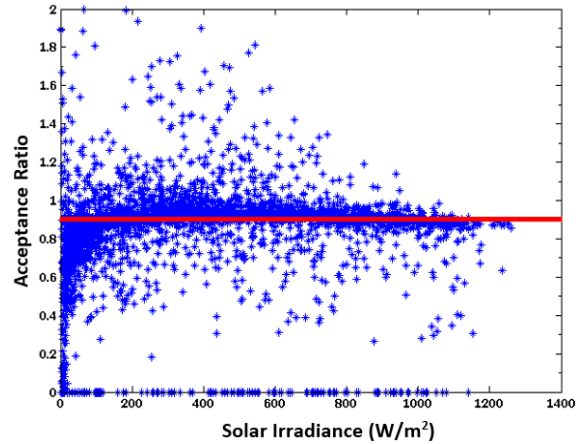


Figure 16. Acceptance ratio in relation to solar irradiance for December 2018

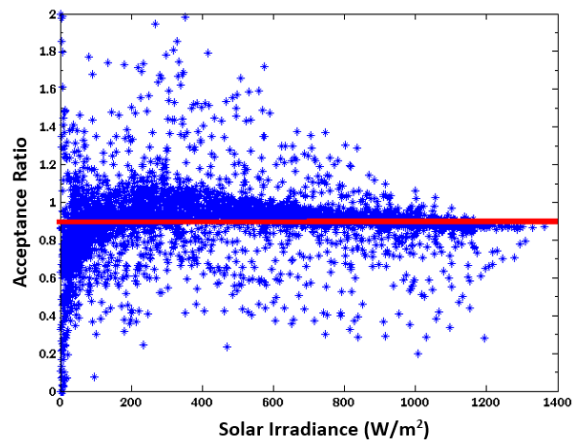


Figure 17. Acceptance ratio in relation to solar irradiance for January 2019

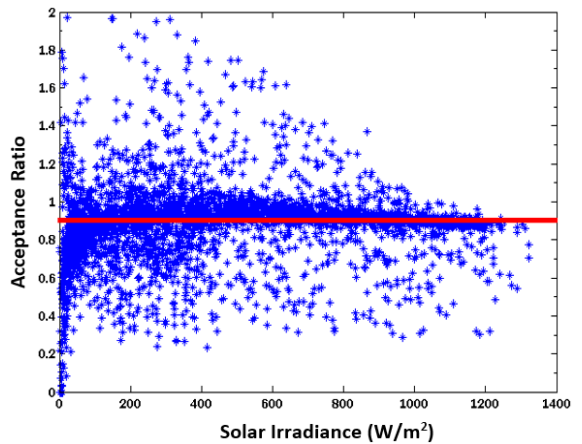


Figure 18. Acceptance ratio in relation to solar irradiance for February 2019

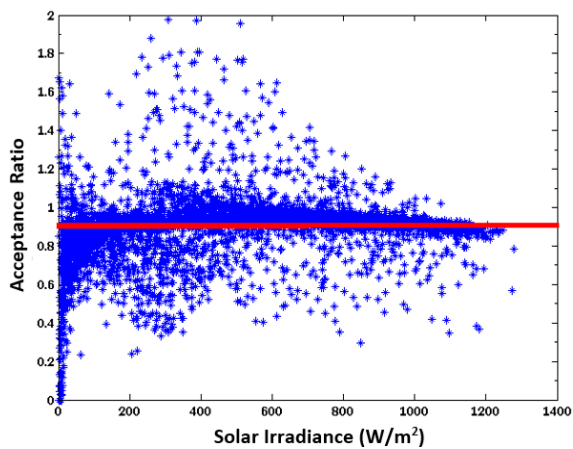


Figure 19. Acceptance ratio in relation to solar irradiance for March 2019

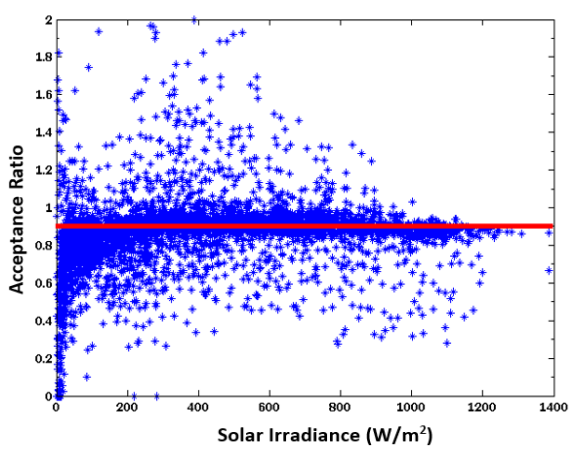


Figure 20. Acceptance ratio in relation to solar irradiance for April 2019

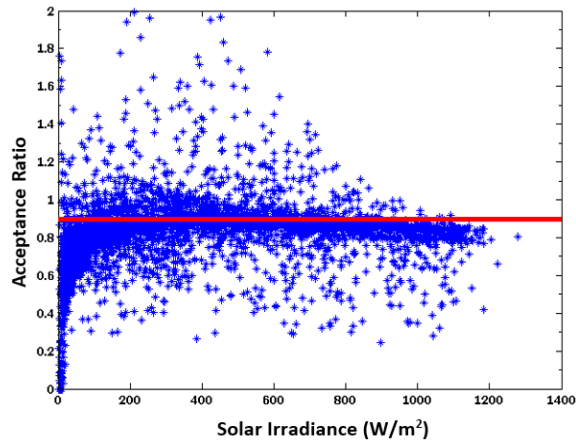


Figure 21. Acceptance ratio in relation to solar irradiance for May 2019

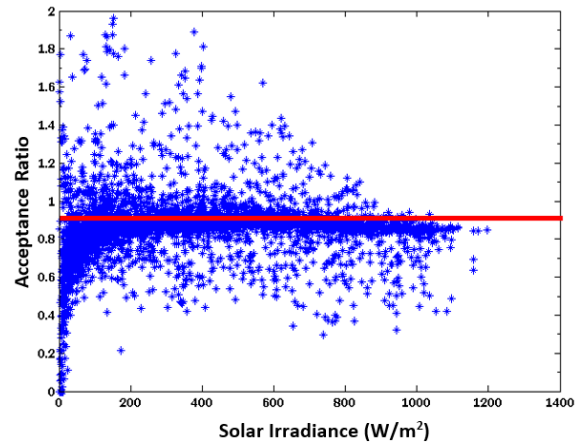


Figure 22. Acceptance ratio in relation to solar irradiance for June 2019

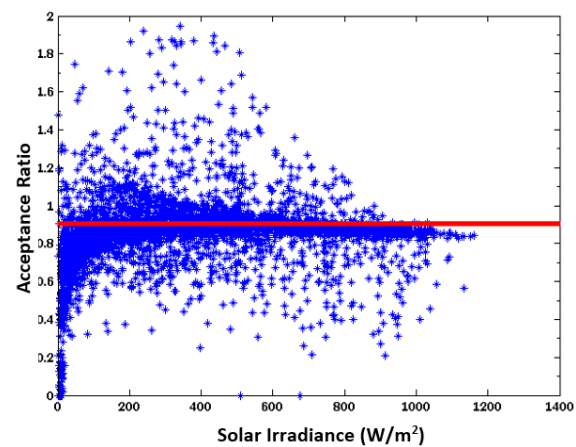


Figure 23. Acceptance ratio in relation to solar irradiance for July 2019

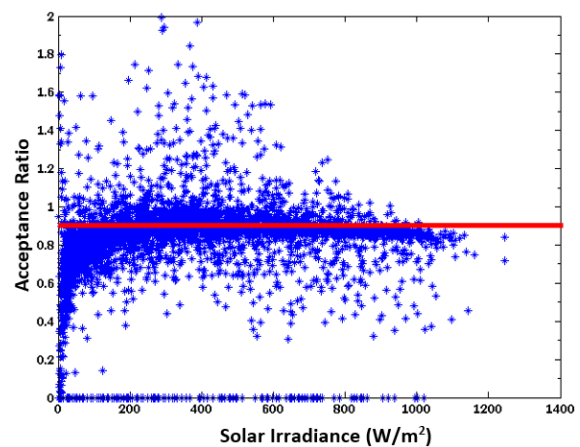


Figure 24. Acceptance ratio in relation to solar irradiance for August 2019

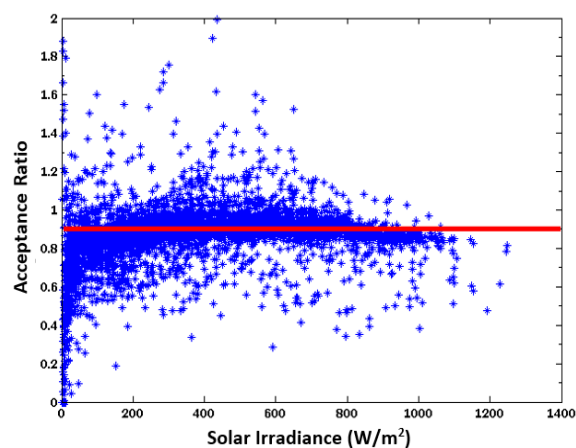


Figure 25. Acceptance ratio in relation to solar irradiance for September 2019

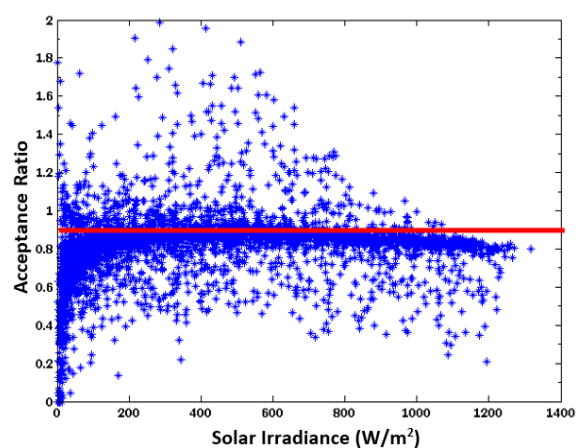


Figure 26. Acceptance ratio in relation to solar irradiance for October 2019

3.2. Yield (Y)

Figure 27 shows a graph combination of actual and predict yield versus month for one-year period. Actual yield is labelled as green bar while predict yield is labelled as red bar. The range of the energy for predict yield is between 0 kWh to 700 kWh. However, none of the actual yield achieved the predicted. The highest actual yield produces energy is only 457.08 kWh.

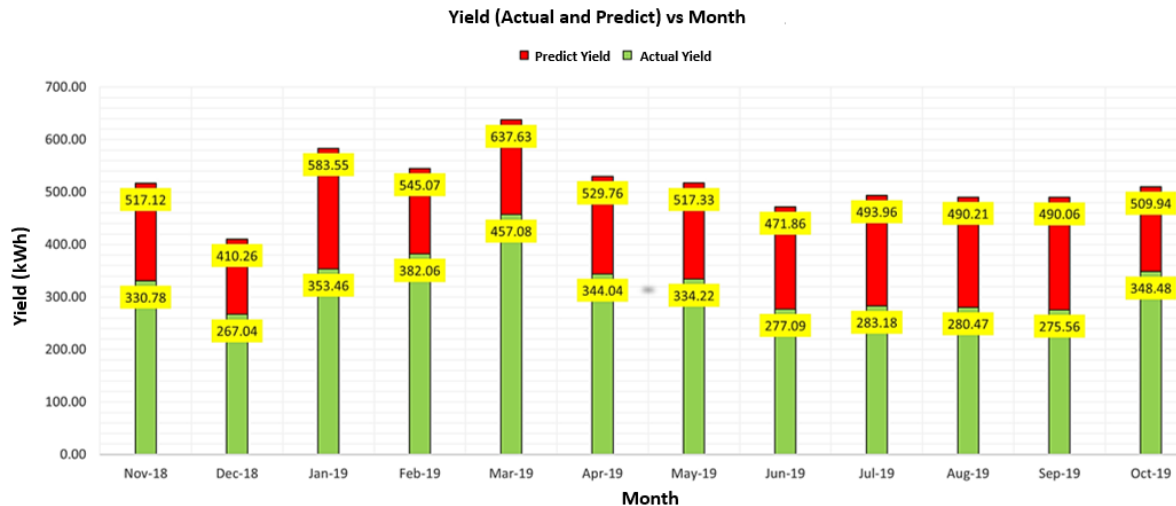


Figure 27. Graph of yield (actual and predict) versus month

3.3. Specific Yield (SY)

Figure 28 shows a graph of actual and predicted specific yield versus month for one-year period. The green bar is actual specific yield, and the red bar is the predicted specific yield. The range of the specific yield is between 0 to 120 kWh(kWp)⁻¹. For predict specific yield, the highest output is in March 2019 which is 117.97 kWh(kWp)⁻¹ and the lowest amount of predict specific yield is in December 2018 which is 75.90 kWh(kWp)⁻¹. Next, the highest amount of actual specific yield which is 84.57 kWh(kWp)⁻¹ in March 2019, and the lowest amount of actual specific yield which is 49.41 kWh(kWp)⁻¹ in December 2018. In conclusion, both actual and predicted specific yield shows the same month at highest and lowest amount produced.

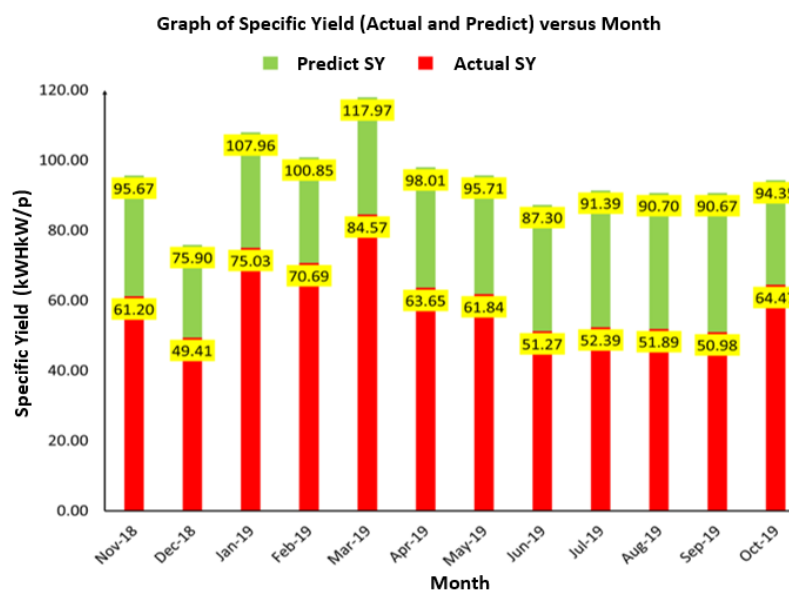


Figure 28. Graph of specific yield (actual and predict) versus month

3.4. Performance ratio (PR)

Figure 29 shows the graph of performance ratio versus months for a one-year period. The purple bar represents performance ratio (PR) and the red dash line is the limit of performance ratio (PR) which is 0.75. Based on Figure 29, PR of the polycrystalline module shows unstable data where in November 2018, the PR is 0.64. A slight increase in December which is 0.65. However, the PR suddenly decreased to 0.61 in January 2019. Increasing amount of PR in February 2019 shows 0.70 and still increase to the highest PR for one year 0.72 in March 2019. After two months of increasing, in April 2019 shows PR decreases to 0.65 and maintained until May 2019. Nevertheless, in June 2019 the PR kept decreasing to 0.59 then 0.57 in July 2019 and August 2019 and dropped to the lowest PR in one year, 0.56 in September 2019. Finally, October 2019 shows a sudden rise of PR to 0.68. Based on data analysis of the performance ratio (PR), none of the data even passes 0.75 as what this polycrystalline GCPV systems should have. Therefore, this system is a low-performance polycrystalline module system.

Table 1 shows the results of calculation of percentage difference of yield, specific yield and performance ratio for each month starting from November 2018 to October 2019. For yield and specific yield, November 2018 started with a high value of percentage difference which is 21.98%. However, the values of percentage difference became unstable from December 2018 to March 2019 cause the percentage difference dropped to 16.49%. Nevertheless, from April 2019 to September 2019, the values of percentage difference rose to 28.02 %. Lastly, in October 2019 the percentage difference of yield decreased to 18.81 %. The performance ratio is critical for determining whether polycrystalline performance is obtainable or needs fixing. The result shows that most of the percentage difference for performance ratio is greater than 10%, indicating that this polycrystalline PV module is defective and must be replaced.

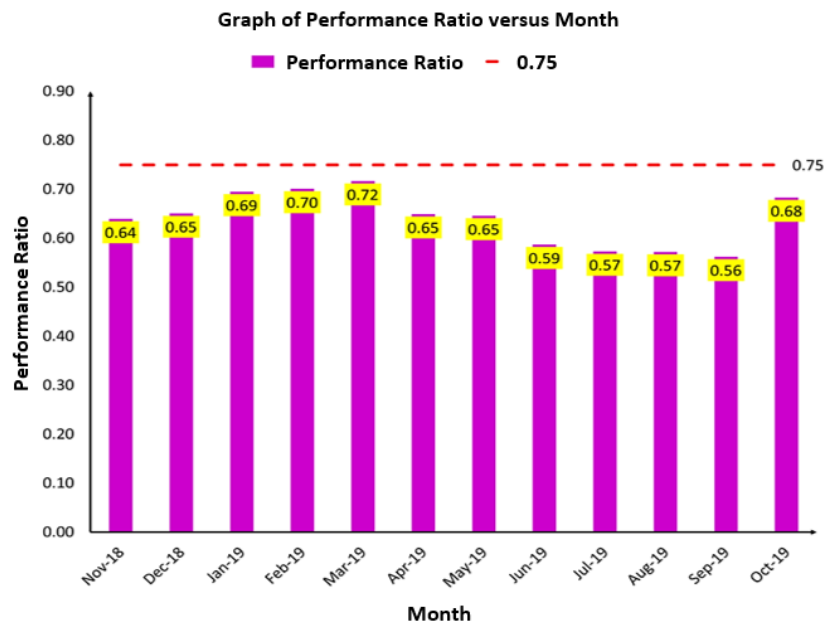


Figure 29. Graph of performance ratio versus month

Table 1. Percentage difference of yield

Month	Percentage difference (%)		
	Yield	Specific yield	Performance ratio
November 2018	21.98	21.97	7.94
December 2018	21.15	21.14	7.07
January 2019	24.56	24.56	10.64
February 2019	17.58	17.58	3.38
March 2019	16.49	16.49	2.26
April 2019	21.25	21.25	7.19
May 2019	21.50	21.50	7.44
June 2019	26.01	26.00	12.17
July 2019	27.12	27.12	13.35
August 2019	27.22	27.22	13.46
September 2019	28.02	28.02	14.30
October 2019	18.81	18.81	4.65

4. CONCLUSION

This study was successful in analyzing the Polycrystalline GCPV systems' P_{ac_actual} and $P_{ac_predict}$. The data from the AR analysis show that the majority of the AR results for the Polycrystalline GCPV system are less than 0.9. Furthermore, the results of the performance ratio show that the overall system is less than 0.75, indicating the worst-case scenario for the GCPV system. These findings confirmed that the GCPV system is operational in the event of a failure. However, more research is needed to determine the significant contribution to a higher cumulative percentage of AR 0.9. Furthermore, a degradation study must be conducted to assess the dependability of the AR indicator in order to confirm the failure of the GCPV system. Finally, the fault analytical approaches of using AC power and AR for early failure detection of GCPV systems were demonstrated to be significant and reliable.

ACKNOWLEDGEMENTS

The authors would like to thank the green energy research centre (GERC) UiTM for their assistance and guidance throughout the project. This research was supported by MARA Research Grant 600-RMC/GPM LPHD 5/3 (150/2021) from Universiti Teknologi MARA.




REFERENCES

- [1] A. Dobrzycki, D. Kurz, and E. Maćkowiak, "Influence of selected working conditions on electricity generation in bifacial photovoltaic modules in polish climatic conditions," *Energies*, vol. 14, no. 16, 2021, doi: 10.3390/en14164964.
- [2] S. Thanasansakorn, T. Thimkrap, and A. Chanyim, "Report On-grid Solar Roof System @ TD," 2022. [Online]. Available: <http://repository.seafdec.or.th/handle/20.500.12067/1758>
- [3] W. Quitiaquez, J. Estupinán-Campos, C. Nieto-Londoño, C. A. Isaza-Roldán, P. Quitiaquez, and F. Toapanta-Ramos, "CFD analysis of heat transfer enhancement in a flat-plate solar collector with different geometric variations in the superficial section," *Int. J. Adv. Sci. Eng. Inf. Technol.*, vol. 11, no. 5, pp. 2039–2045, 2021, doi: 10.18517/IJASEIT.11.5.15288.
- [4] N. A. A. Jamil, S. A. Jumaat, S. Salimin, M. N. Abdullah, and A. F. M. Nor, "Performance enhancement of solar powered floating photovoltaic system using arduino approach," *Int. J. Power Electron. Drive Syst.*, vol. 11, no. 2, pp. 651–657, 2020, doi: 10.11591/ijpeds.v11.i2.pp651-657.
- [5] D. Singh, and R. S. Kathuria, "Fault prediction and analysis techniques of solar cells and pv modules," *Int. J. Eng. Sci. Res. Technol.*, vol. 7, no. 8, pp. 384–399, 2018.
- [6] K. Kawasaki, and K. Okajima, "A Method for the detection of decrease in power in PV systems using satellite data," *Smart Grid Renew. Energy*, vol. 10, no. 01, pp. 1–15, 2019, doi: 10.4236/sgre.2019.101001.
- [7] F. A. M. Shukor, H. Zainuddin, N. Muhammad, and F. L. M. Khir, "Acceptance ratio analysis: an early fault indicator for grid-connected photovoltaic system," *Int. J. Adv. Sci. Eng. Inf. Technol.*, vol. 11, no. 3, pp. 1214–1223, 2021, doi: 10.18517/ijaseit.11.3.12614.
- [8] M. A. Islam, M. Hasanuzzaman, and N. A. Rahim, "Experimental investigation of on-site degradation of crystalline silicon PV modules under Malaysian climatic condition," *Indian J. Pure Appl. Phys.*, vol. 56, no. 3, pp. 226–237, 2018.
- [9] I. Mustapha, M. K. Dikwa, B. U. Musa, and M. Abbagana, "Performance evaluation of polycrystalline solar photovoltaic module in weather conditions of Maiduguri, Nigeria," *Arid Zo. J. Eng.*, vol. 9, no. October, pp. 69–81, 2013.
- [10] J. G. Narvaez, D. C. Ceballos, J. M. Manzano, and S. R. Sarsoza, "Analysis of electric power consumption and proposals for energy sustainability for the University of Ucodecauca (Colombia)," *Int. J. Adv. Sci. Eng. Inf. Technol.*, vol. 10, no. 3, pp. 1107–1116, 2020, doi: 10.18517/ijaseit.10.3.10812.
- [11] N. Muhammad, H. Zainuddin, E. Jaaper, and Z. Idrus, "An early fault detection approach in grid-connected photovoltaic (GCPV) system," *Indones. J. Electr. Eng. Comput. Sci.*, vol. 17, no. 2, 2019, doi: 10.11591/ijeecs.v17.i2.pp671-679.
- [12] C. Chávez, J. D. Ramírez, F. T. L. María, P. Otero, S. Taco-Vásquez, and V. Tibanlombo, "Determination of the appropriate number of photovoltaic panels for microgeneration and self-supply of final consumers by energy production estimation via fuzzy logic," *Int. J. Adv. Sci. Eng. Inf. Technol.*, vol. 12, no. 2, pp. 460–469, 2022, doi: 10.18517/ijaseit.12.2.15291.
- [13] V. Prada, O. I. Caldas, E. Mejía-Ruda, M. Mauleudoux, and O. F. Avilés, "Modeling and simulation of a DC micro-grid with a model predictive controller," *Int. J. Adv. Sci. Eng. Inf. Technol.*, vol. 10, no. 3, pp. 1091–1098, 2020, doi: 10.18517/ijaseit.10.3.11343.
- [14] S. Suraj, J. J. Jijesh, and S. Soman, "Analysis of dual phase dual stage boost converter for photovoltaic applications," *Int. J. Adv. Sci. Eng. Inf. Technol.*, vol. 10, no. 3, pp. 920–928, 2020, doi: 10.18517/ijaseit.10.3.5346.
- [15] S. Ekici and M. A. Kopru, "Investigation of PV system cable losses," *Int. J. Renew. Energy Res.*, vol. 7, no. 2, pp. 807–815, 2017.
- [16] P. Sathyanarayana, R. Ballal, L. P. Sagar S, and G. Kumar, "Effect of shading on the performance of solar PV panel," vol. 5, no. 1A, pp. 1–4, 2015, doi: 10.5923/c.ep.201501.01.
- [17] L. Q. Thai, and A. T. H. T. Anh, "Design a photovoltaic simulator system based on two-diode model with linear interpolation method," *Int. J. Power Electron. Drive Syst.*, vol. 13, no. 2, pp. 856–864, 2022, doi: 10.11591/ijpeds.v13.i2.pp856-864.
- [18] K. G. P. Pratama, H. Hermawan, and T. Andromeda, "Analysis performance of grid tie photovoltaic type polycrystalline using solar irradiance simulation," *E3S Web Conf.*, vol. 125, no. 2019, 2019, doi: 10.1051/e3sconf/201912514013.
- [19] N. Sapountzoglou, and B. Raison, "A grid connected pv system fault diagnosis method," *Proc. IEEE Int. Conf. Ind. Technol.*, vol. 2019-Febru, pp. 977–982, 2019, doi: 10.1109/ICIT.2019.8755166.
- [20] D. Nilsson, "Fault detection in photovoltaic systems," thesis, KTH Vetenskap och Konst, Sweden, 2015. [Online]. Available: <https://www.diva-portal.org/smash/get/diva2:754340/FULLTEXT01.pdf>
- [21] P. N. A. M. Yunus, S. I. Sulaiman, and A. M. Omar, "Online performance monitoring of grid-connected photovoltaic system using hybrid improved fast evolutionary programming and artificial neural network," *Indones. J. Electr. Eng. Comput. Sci.*, vol. 8, no. 2, pp. 399–406, 2017, doi: 10.11591/ijeecs.v8.i2.pp399-406.
- [22] C. Kara Mostefa Khelil, B. Amrouche, A. soufiane Benyoucef, K. Kara, and A. Chouder, "New intelligent fault diagnosis (IFD) approach for grid-connected photovoltaic systems," *Energy*, vol. 211, pp. 1–18, 2020, doi: 10.1016/j.energy.2020.118591.




- [23] A. Tjahjono, A. Rofiq, M. H. Faiz, and D. O. Anggriawan, "Global maximum power point tracking of PV array under non-uniform irradiation condition using adaptive velocity particle swarm optimization," *Int. J. Adv. Sci. Eng. Inf. Technol.*, vol. 10, no. 2, pp. 888–898, 2020, doi: 10.18517/ijaseit.10.2.11610.
- [24] H. Zainuddin, S. Shaari, A. M. Omar, S. I. Sulaiman, Z. Mahmud, and F. Muhamad Darus, "Prediction of module operating temperatures for free-standing (FS) photovoltaic (PV) system in Malaysia," *International Review on Modelling and Simulations*, vol. 4, no. 6, pp. 3388–3394, 2011.
- [25] N. H. Bostamam, H. Zainuddin, and S. I. Sulaiman, "Module operating temperature model for free-standing photovoltaic system in Malaysia using principal component regression," *Int. J. Simul. Syst. Sci. Technol.*, vol. 17, no. 41, pp. 53.1–53.6, 2016, doi: 10.5013/IJSSST.a.17.41.53.
- [26] A. R. Amelia, Y. M. Irwan, W. Z. Leow, M. Irwanto, I. Safwati, and M. Zhafarina, "Investigation of the effect temperature on photovoltaic (PV) panel output performance," *Int. J. Adv. Sci. Eng. Inf. Technol.*, vol. 6, no. 5, pp. 682–688, 2016, doi: 10.18517/ijaseit.6.5.938.
- [27] F. Faraz Ahmad, Z. Said, and A. Amine Hachicha, "Experimental performance evaluation of closed loop mist/fog cooling system for photovoltaic module application," *Energy Convers. Manag.*, vol. 14, no. March, p. 100226, 2022, doi: 10.1016/j.ecmx.2022.100226.
- [28] J. Gosumbonggot and G. Fujita, "Global maximum power point tracking under shading condition and hotspot detection algorithms for photovoltaic systems," *Energies*, vol. 12, no. 5, 2019, doi: 10.3390/en12050882.
- [29] K. A. Kim, G. S. Seo, B. H. Cho, and P. T. Krein, "Photovoltaic hot-spot detection for solar panel substrings using AC parameter characterization," *IEEE Trans. Power Electron.*, vol. 31, no. 2, pp. 1121–1130, 2016, doi: 10.1109/TPEL.2015.2417548.
- [30] M. Dhimish, V. Holmes, B. Mehrdadi, M. Dales, and P. Mather, "Photovoltaic fault detection algorithm based on theoretical curves modelling and fuzzy classification system," *Energy*, vol. 140, pp. 276–290, 2017, doi: 10.1016/j.energy.2017.08.102.
- [31] S. Samara and E. Natsheh, "Intelligent PV panels fault diagnosis method based on NARX network and linguistic fuzzy rule-based systems," *Sustain.*, vol. 12, no. 5, 2020, doi: 10.3390/su12052011.
- [32] S. M. Ruiz, M. V. Chamorro, G. V. Ochoa, J. F. Villegas, and C. A. Peñaloza, "Effects of environmental conditions on photovoltaic generation system performance with polycrystalline panels," *Int. J. Adv. Sci. Eng. Inf. Technol.*, vol. 11, no. 5, pp. 2031–2038, 2021, doi: 10.18517/IJASEIT.11.5.9335.
- [33] N. S. Baghel and N. Chander, "Performance comparison of mono and polycrystalline silicon solar photovoltaic modules under tropical wet and dry climatic conditions in east-central India," *Clean Energy*, vol. 6, no. 1, pp. 929–941, 2022, doi: 10.1093/ce/zkac001.

BIOGRAPHIES OF AUTHORS






Nurmalessa Muhammad    is a lecturer in Department of Physics and Material, Faculty of Applied Sciences since 2008 at the Universiti Teknologi MARA, Selangor, Malaysia. She received her Bachelor's in Physics (Hons) and PhD in Photovoltaics System from Universiti Teknologi MARA in 2006 and 2020, respectively. She obtained her MSc. Energy Technology from Universiti Kebangsaan Malaysia in 2011. Her research interest including the field of photovoltaic systems, energy audit, sustainable energy, renewable energy, and failure detection on photovoltaic systems. She can be contacted at email: nurmalessa@uitm.edu.my.



Fiona Roland    is now under MyReskill Workforce (Industrial Upskilling)–Product and Test Engineering program handle by USAINS Holding Sdn. Bhd. She received the bachelor's degree in science physics from Universiti Teknologi MARA, Shah Alam, Malaysia. Her final year project is fault detection on Polycrystalline Grid-Connected Photovoltaics system of AC power output. She can be contacted at email: fionamit12@gmail.com.



Hedzlin Zainuddin    received her B. Sc in Physics from Universiti Kebangsaan Malaysia in the year 2000. She obtained her M. Sc in Photovoltaics Energy System from the same university in the year 2003. In 2014, she completed her Ph. D in photovoltaics from Universiti Teknologi MARA, Shah Alam, Malaysia. Her specialization areas are physics, solar photovoltaic (PV) field testing, design of grid-connected PV (GCPV) system, design of off-grid PV (OGPV) system, mathematical and computational modeling (linear, multiple linear and artificial intelligent) and PV system fault detection. She presently holds four certificates of competency in GCPV and OGPV. She has been working with Industries and Government Agencies for 13 years since 2007 through consultation projects. She can be contacted at email: hedzl506@uitm.edu.my.